 

PACS numbers: 42.60.Mi; 42.79.Ta
DOI: 10.1070/QE2008v038n11ABEH013755

# Control of nonstationary multimode lasing by neural networks with radius basis functions

V.I. Ledenev

***Abstract*. A neural network with radius basis functions is trained by using the evolution approach to recognise the mode characteristics of a Fabry – Perot resonator. It is shown that the network is capable of determining simultaneously the qualitative and quantitative characteristics of nonstationary lasing. The efficiency of the approach for determining the amplitudes of the fundamental and first modes on passing from single-mode to two-mode lasing is demonstrated by the example of a network with the response time shorter than the resonator round-trip transit time. The efficiency of a new scheme, in which field-amplitude detectors are located inside the resonator outside of the output aperture, is also demonstrated.**

***Keywords***: *laser, Fabry – Perot resonator, lasing dynamics, numerical simulation, neural network.*

## 1. Introduction

The development of methods for controlling nonstationary multimode lasing is of current interest because this provides the relation between the theory of such lasing [1 – 3] and experimental data and also because higher-order modes are often used in modern laser technologies [4]. In [5], it was proposed to use a classical three-level neural network for determining qualitative characteristics of lasing. A part of an optical beam in a scheme used in [5] was directed to field-amplitude detectors. The output data set was obtained after the normalisation of signals from $N_i$ detectors to their maximum value. As a result, the three-level network was capable of recognising passages between regimes with different numbers of generated modes (single-mode or two-mode lasing). The passage could be recognised when the pump rate only slightly exceeded the threshold rate for the given type of lasing. Such a scheme for lasing control can be useful when an autonomous device is required for determining the number of generated modes.

The scheme used in [5] has a number of disadvantages. First, it does not allow the measurement of mode amplitudes, which is important for theoretical studies and practical applications. Second, a beamsplitter in this scheme is located in the near-field radiation zone, whereas it is preferable to place into the beam only elements controlling radiation. Third, this scheme has a considerable training time, especially in the case of many situations to be recognised by the network (in the case of many network outputs).

This study eliminated these disadvantages to a great extent. As in [5], it is assumed in this paper that transverse radiation intensity distributions in the output aperture plane have specific features from which the number of generated modes, their amplitudes, and phase relations can be determined. The construction of a neural network capable of recognising both qualitative and quantitative parameters (amplitudes of generated modes) of lasing is considered. Thus, information on mode phases is excluded from consideration, which simplifies training by retaining the general approach. In the general case the number of situations recognised by the network can be estimated as the number of generated modes multiplied by the number of discretization levels of the field amplitude and the number of discretization levels of the phase of each of the modes.

In this paper, a new arrangement of field-amplitude detectors was used. Unlike [5], they were placed inside the resonator in the output aperture plane outside the aperture (Fig. 1).

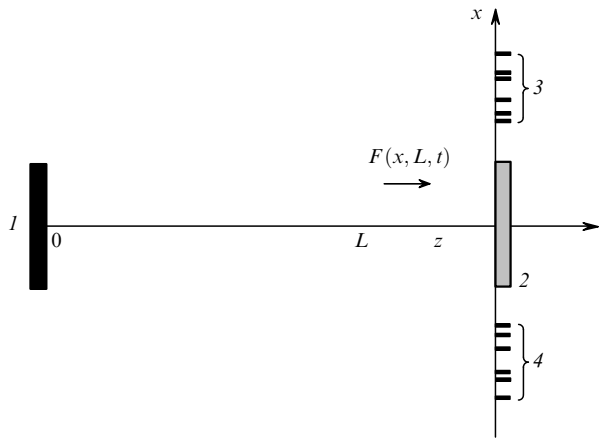


**Figure 1.** System for controlling the mode composition of laser radiation: (*1*) highly reflecting mirror and active medium layer; (*2*) output mirror; (*3*, *4*) field-amplitude detectors (located symmetrically and non-equidistantly); $F(x, L, t)$ is the amplitude of a wave incident on the output mirror and detectors.

**V.I. Ledenev** Institute on Laser and Information Technologies, Russian Academy of Sciences, Svyatoozerskaya ul. 1, 140700 Shatura, Moscow region, Russia; e-mail: ledenev_ilit@rambler.ru

Received 8 November 2007; revision received 11 April 2008
*Kvantovaya Elektronika* **38** (11) 1033 – 1038 (2008)
Translated by M.N. Sapozhnikov

A neural network with radius basis functions (NRBF) was selected as an object for training. This choice was made because this network can be rapidly trained [6] and can be expanded to recognise new situations without changing previously determined weight factors. The evolution training algorithm was used which is based on the recognition of predetermined distributions by the NRBF (controllable training) [5, 6]. The training set was constructed in [5] by using the eigenfunctions of a Fabry–Perot resonator without an active medium, which were found numerically. This simplification gave good results because it was necessary to recognise only qualitative parameters of lasing. However, the NRBF training for determining quantitative lasing parameters (mode amplitudes) based on the eigenfunctions of the empty resonator proved to be unsatisfactory. The training set was constructed in the present paper by using the eigenfunctions of the Fabry–Perot resonator, which were obtained by solving a separate problem of the development of generation in a laser with a medium having an instant nonlinear response. Although this approach is also simplified, it led to satisfactory results.

## 2. The model of lasing

The NRBF operation was investigated based on the numerical model of nonstationary lasing [5, 7]. In a planar geometry in the small-angle approximation of the scalar diffraction theory, the electric field $E$ in the resonator was represented in the form of counterpropagating plane waves modulated by smooth envelopes:

$$E(x,z,t) = [F(x,z,t)\exp(\mathrm{i}k_0 z) + B(x,z,t)\exp(-\mathrm{i}k_0 z)]\exp(-\mathrm{i}\omega_0 z). \quad (1)$$

Here, $\omega_0$ is the carrier frequency; $k_0 = \omega_0/c$; the $z$ axis is directed along the beam propagation, and the $x$ axis is perpendicular to this direction. The dynamics of the envelopes of the forward $[F(x,z,t)]$ and backward $[B(x,z,t)]$ waves was described by the equations

$$2\mathrm{i}k_0\left(\frac{1}{c}\frac{\partial B}{\partial t} - \frac{\partial B}{\partial z}\right) + \frac{\partial^2 B}{\partial x^2} - \mathrm{i}k_0 g B = 0, \quad (2)$$

$$2\mathrm{i}k_0\left(\frac{1}{c}\frac{\partial F}{\partial t} + \frac{\partial F}{\partial z}\right) + \frac{\partial^2 F}{\partial x^2} - \mathrm{i}k_0 g F = 0, \quad (3)$$

where $g$ is the radiation gain. Because field-amplitude detectors were located in the $z = L$ plane in the region $|x| > R$, where $R$ is the radius of resonator mirrors, it is convenient to solve equations (2) and (3) by the spectral method (in [5], the field was determined only on resonator mirrors by calculating the Fresnel–Kirchhoff integral). The number of elements was 8192, while the number of elements on the mirror was 512. The waves on resonator mirrors satisfied the reflection conditions:

$$F(x,0,t) = -B(x,0,t)r_1, \quad (4)$$

$$B(x,L,t) = -F(x,L,t)r_2. \quad (5)$$

Here, $r_1$ and $r_2$ are the amplitude reflectances of the highly reflecting and output mirrors, respectively. The equation for the radiation gain $g$ in the active medium included processes of simulated emission and relaxation with the time constant $\tau$:

$$\tau\frac{\partial g}{\partial t} = g_0 - g(1 + |F|^2 + |B|^2). \quad (6)$$

Equation (6) was solved by using the implicit scheme of the second-order approximation.

As the initial condition for determining the mode composition of the unfilled resonator, the superposition of distributions found with the help of analytic expressions was used [8], while the initial condition for problem (2)–(6) was the superposition of the eigenfunctions found for the medium with an instant nonlinear response.

The normalised eigenfunctions $U_j$ of the resonator were determined in the output mirror plane with an error of $\delta_j \lesssim 10^{-14}$ according to the criterion $\delta_j = ||\hat{P}U_j - \gamma_j U_j||$ [9]. Here, $\gamma_j$ are the eigenvalues of the operator $\hat{P}$ of the round-trip transit for radiation in the resonator. The transition from single-mode to two-mode lasing was simulated by specifying the initial condition for the forward wave with the amplitude $F(x,0,0)$ with the help of the distribution of the fundamental mode $U_0(x)$ of the resonator. The initial condition for the backward wave with the amplitude $B(x,0,0)$ was determined after a round-trip transit of radiation in the resonator.

The complex amplitudes of the fundamental and first mode were found by expanding $F$ in the $z = L$ plane:

$$F(x,L,t) = a(t)U_0(x) + b(t)U_1(x). \quad (7)$$

Time-dependent coefficients $a(t)$ and $b(t)$ were found by integration within the aperture, i.e. from $-R$ to $R$:

$$a(t) = \frac{\int_{-R}^{R} F(x,L,t)U_0^*(x)\mathrm{d}x}{\int_{-R}^{R} U_0(x)U_0^*(x)\mathrm{d}x}, \qquad b(t) = \frac{\int_{-R}^{R} F(x,L,t)U_1^*(x)\mathrm{d}x}{\int_{-R}^{R} U_1(x)U_1^*(x)\mathrm{d}x}. \quad (8)$$

The centre of gravity of the far-field angular power distribution was calculated from the expression

$$E_\mathrm{f}(t) = \frac{\int_{-\infty}^{\infty} \vartheta W(\vartheta,t)\mathrm{d}\vartheta}{\int_{-\infty}^{\infty} W(\vartheta,t)\mathrm{d}\vartheta}, \quad (9)$$

where

$$W(\vartheta,t) = \frac{k_0}{2\pi}\left|\int_{-\infty}^{\infty} F(x,L,t)\exp(-\mathrm{i}k_0\vartheta x)\mathrm{d}x\right|^2. \quad (10)$$

Calculations were performed for a Fabry–Perot resonator with parameters coinciding with those of the resonator used in [5, 7]. The radius $R$ of the resonator mirrors was 1 cm, the distance between the mirrors was $L = 150$ cm, and mirror reflectances were $r_1 = 1$ and $r_2 = 0.8$. The Fresnel number of the resonator was $N_\mathrm{F} = 6.25$. The active medium was a thin layer adjacent to the highly reflecting mirror and had the relaxation time $\tau = 6.0 \times 10^{-6}$ s. Figure 2a shows the dependences $|a(t)|$ and $|b(t)|$ obtained for the pump excess over the threshold

$k = g_0/g_t = 1.4801$ (the small-signal gain $g_0$ exceeded the threshold gain for the third mode). For this set of parameters, the fundamental mode had time to relax to the stationary state during the first 40 μs of lasing. By the instant $t = 44$ μs, the amplitude of the first mode achieved a noticeable value and relaxation oscillations of both modes appeared, resulting in the establishment of the regime of beating of the fundamental and first transverse modes. The dependence of $E_f(t)$ is presented in Fig. 2b. The centre of gravity of the far-field angular power distribution in the beating regime oscillated with a period of 0.39 μs (Fig. 2c). A comparison of the envelope in Fig. 2b with the dependence $|b(t)|$ in Fig. 2a shows that they have close shapes.

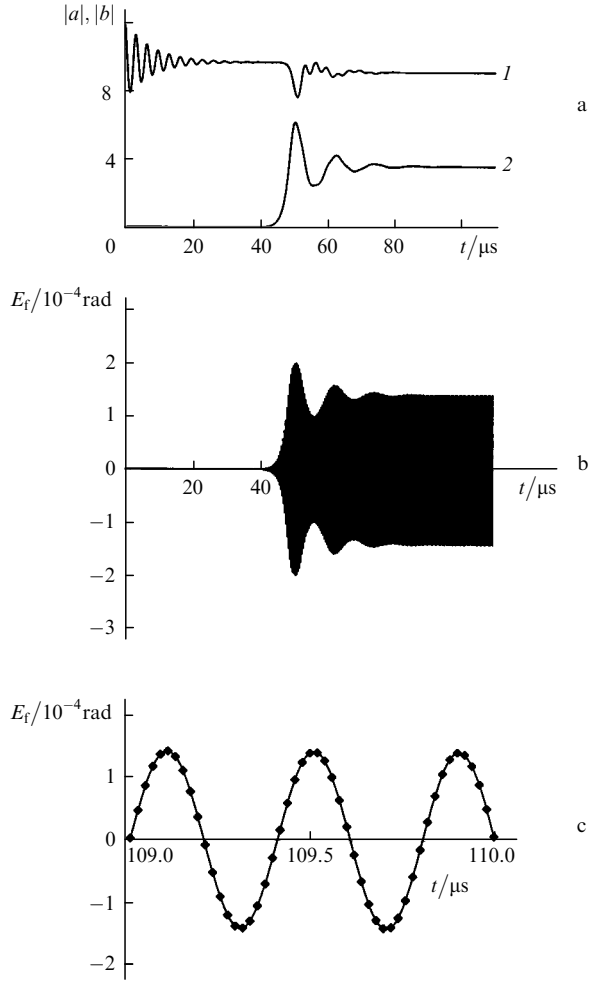


**Figure 2.** Transition from single-mode to two-mode lasing: amplitudes of the fundamental (*1*) and first (*2*) modes calculated by expressions (8) (a); the time dependence of the position of the centre of gravity of the far-field angular power distribution calculated by expressions (9) and (10) (b); and oscillations of this centre of gravity established at the 109th microsecond from the beginning of the establishment process (c).

The determination of lasing parameters in this case was a complicated test problem for the NRBF: in the case of single-model lasing, the recognition of the oscillation amplitude of the fundamental mode required a great number of neural network outputs, while in the case of two-mode lasing the recognition of the oscillation amplitude of one mode occurred for comparable variations in the oscillation amplitude of another mode.

The extrapolation of distributions of the eigenfunctions $U_j$, defined for $z = L$ and $|x| < R$, to the region $|x| > R$ was found by calculations per a round-trip transit in the resonator. The field-amplitude detectors were mounted so that the moduli of superpositions $|a_p U_0(x_d) + b_q U_1(x_d)| = |U_d|$ required for the network training were maximally different in the locations $x = x_d$ of detectors for the chosen values (classes) $a_p > 0$, $b_q \geqslant 0$, where $p = 1, 2, ..., N_p$, $q = 1, 2, ..., N_q$, $N_p$, $N_q$ where $N_p$ and $N_q$ are the numbers of discretization levels of the amplitude. As a result, detectors were arranged non-equidistantly along the $x$ axis, but symmetrically with respect to the $z$ axis of the resonator. The ranges of values of $a_p$ and $b_q$ covered the ranges of variation of $|a(t)|$ and $|b(t)|$, respectively. The discretization with a constant step $\Delta a = a_{p+1} - a_p = \text{const}$, $\Delta b = b_{q+1} - b_q = \text{const}$ was used.

One of the training sets is shown in Fig. 3. Detectors with numbers $i = 1 - 12$ were mounted over the output mirror, while detectors with $i = 13 - 24$ were located under this mirror. The training to recognise lasing at one fundamental mode and to determine $|a(t)|$ was performed by using symmetric distributions. In this case, signal intensities on detectors closest to the output mirror differed by $\sim 35\,\%$, this difference decreasing with distance from the mirror (Fig. 3a). The training to recognise two-mode lasing and to determine $|a(t)|$ and $|b(t)|$ was performed by using asymmetric distributions. Signal intensities on the upper detector closest to the output mirror differed by $\sim 44\,\%$, this difference increasing away from the mirror (Fig. 3b). Signal intensities on detectors located under the mirror strongly varied depending on the detector number (Fig. 3b).

The problem facing the NRBF is to determine $|a(t_n)|$ and $|b(t_n)|$ from the values of $|F(x_d, L, t_n)|$ for $|x_d| > R$ for each the $t_n$th round-trip transit of radiation in the resonator. In the case of two-mode lasing, the NRBF should in fact solve the inverse problem of determining the moduli of complex amplitudes from the modulus of the sum of their complex distributions at detector locations.

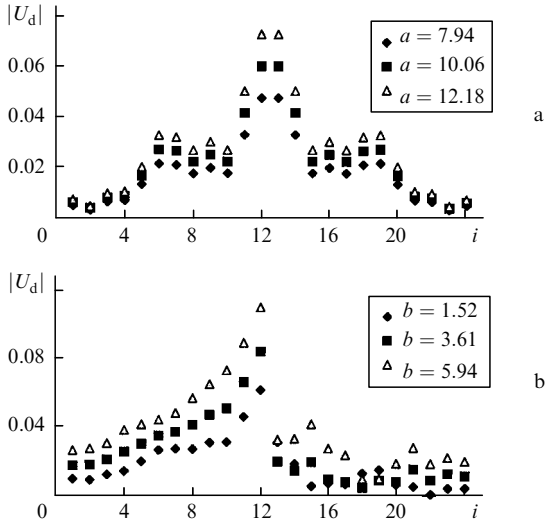


**Figure 3.** Elements of the training set for the fundamental mode in the cases of single-mode lasing (different distributions correspond to different outputs of the neural network) (a) and two-mode lasing (all tree distributions should have the same output of the neural network, corresponding to the fundamental-mode amplitude 7.67) (b).

## 3. Neural network with radius basis functions

The NRBF (Fig. 4) consisted of three layers: the input or detector layer (with elements numbered by the subscript $i$), the example layer (with elements numbered by subscripts $m$ or $l$), and the summation layer (with elements numbered by the subscript $k$). The number of neurons at the input is $N_i = 24$. Radiation detectors in the input layer were assumed point detectors. The number of neurons in the second layer was equal to the number of examples, while the number of neurons in the summation layer (the number of classes) was equal to the number of amplitude discretization levels. The weights $w_{im}$ of the $m$th neuron in the example layer were set equal to the components of the input vector of the corresponding example. The weights $w_{mk}$ of the $k$th neuron in the summation layer were determined during training. The $k$th output of the network should give the value 1 if the distribution corresponding to the class being determined is supplied to the input. The rest of the outputs should give in this case the value 0.

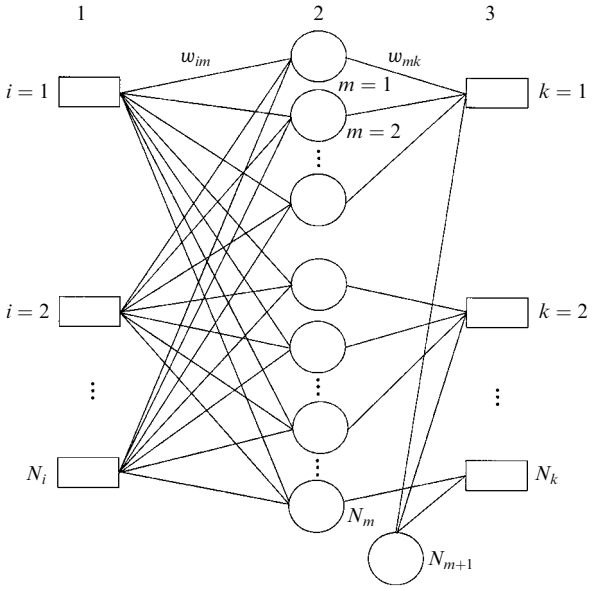


**Figure 4.** Neural network with radius basis functions: (*1*) detector layer; (*2*) example layer; (*3*) summation layer; element $N_{m+1}$ has the output equal to $-1$ and is used to produce a displacement in neurons of layer 3.

When a field distribution $X_i$, produced, for example, during nonstationary lasing, was incident on detectors, the input of the $m$th neuron in the example layer was determined from the expression

$$d_m = \sqrt{\sum_{i=1}^{N_i} (w_{im} - X_i)^2}\,. \tag{11}$$

The output of the $m$th neuron in this layer was described by the Gaussian

$$y_m = \exp(-d_m^2/s_m). \tag{12}$$

The two variants of the NRBF were studied. In the first case, the radii $s_m$ of covers formed the matrix $\hat{s}_{ml}$ ($m, l = 1, 2, ..., N_m$):

$$\hat{s}_{ml} = \alpha \sqrt{\sum_{i=1}^{N_i} (w_{im} - w_{il})^2}\,, \quad \hat{s}_{mm} = \min_{m, l \neq m} \hat{s}_{ml}, \tag{13}$$

where $\alpha > 0$ is a number specified before training. In the second case, the radii of covers formed the vector $\boldsymbol{s}$ from $m$ elements. The input of the $k$th neuron in the summation layer was described (in the first case, for each column of the matrix $\hat{s}_{ml}$) by the expression

$$X_k = \sum_{m=1}^{N_m} w_{mk} y_m - y_{0k},$$

where $y_{0k}$ is the displacement at the input of the $k$th neuron. The response of the $k$th neuron of the summation layer was described by the sigmoid function [6]

$$y_k = \frac{1}{1 + \exp(-X_k)}.$$

In these two cases the neural networks with the same number of outputs behaved differently during training. The time during which the root-mean-square deviation of the network outputs from samples achieved $\sim 10^{-12}$ (training time) for $\alpha \ll 1$ in (13) for the first variant of the neural network was a few tens of seconds and was considerably shorter than the training time for the second variant of the neural network for small radii of covers. For $\alpha \sim 1$, several hours were required to train the NRBF. Because in the first case the neural network for the specified input set $X_i$ could produce $N_m$ outputs by using different columns of the matrix $\hat{s}_{ml}$, all columns with $l = 1, ..., N_m$ were used to recognise lasing parameters and a variant with the output closest to 1 was chosen.

In the second case, the NRBF for the specified input set $X_i$ had one output corresponding to the chosen values $s_m$. One can see from Fig. 4 that neural networks could also differ in the number of examples combined to represent one amplitude discretization level. We studied NRBFs with the number of classes from 4 to 35. Below, the typical NRBF is considered, which was constructed by parts, with the number of elements $N_i = 24$, $N_m = 35$, $N_k = 35$ and $\alpha \sim 1$ for the fundamental mode in the case of single-mode lasing; with $N_m = 25$, $N_k = 25$ and $\alpha \ll 1$ for the first mode in the case of two-mode lasing; and with $N_m = 20$, $N_k = 4$, $\alpha \ll 1$ for the fundamental mode in the case of two-mode lasing.

The training set for the NRBF consisted of three groups of examples. The first group included distributions $a_m |U_0(x_d)|$ ($m = 1, 2, ..., N_m$) intended for training the first part of the NRBF to recognise the generation of one fundamental mode and to determine $|a(t_n)|$. The second group contained distributions $|a_s U_0(x_d) + b_m \times U_1(x_d)|$ ($a_s$ is the stationary value of the fundamental mode amplitude) on which the second part of the neural network was trained to determine $|b(t_n)|$ in the case of two-mode lasing. The fundamental mode amplitude was not recognised in this case. Finally, the third group included distributions $|a_k U_0(x_d) + b_q U_1(x_d)|$ ($k = 1, 2, ..., N_k, q = 1, 2, ..., N_q$, $N_k = 4$, $N_q = 5$) on which the third part of the neural network was trained to determine $|a(t_n)|$ in the case of two-mode lasing. The first mode amplitude was not recognised in this case. Each of the parts of the network was trained independently of other parts.

The combination of the parts to one network was performed by combining successively examples and combining outputs in the corresponding layers. No new connections were established in this case. Thus, we can assume that each of the parts of the NRBF completed the already trained network, and the recognition of lasing parameters by the entire network did not differ from the recognition of these parameters by each of its parts.

## 4. Determination of the qualitative and quantitative lasing parameters

Figure 5 shows lasing parameters for one fundamental mode recognised by the neural network. One can see that the NRBF reliably determines the lasing amplitude up to $t = 44$ μs. The deviation of the values determined by the network from those obtained by expression (9) does not exceed 6 % (Fig. 5b). After that, all the outputs of the network give zeroes, which means that lasing at one fundamental mode ceases.

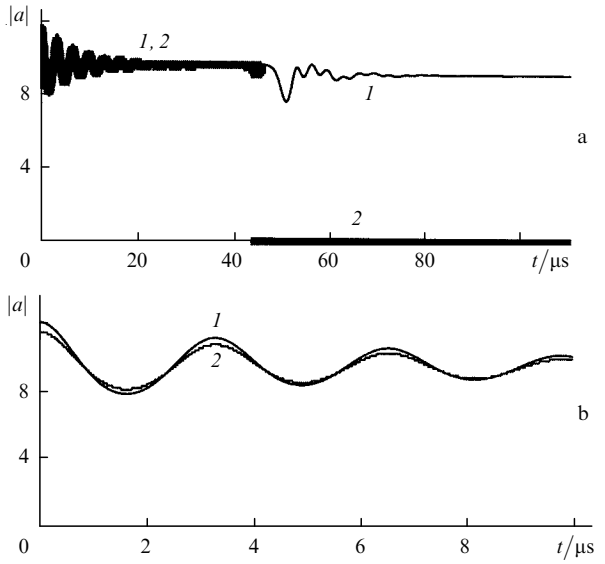


**Figure 5.** Determination of qualitative lasing parameters of one fundamental mode (a) and the amplitude of this mode (b): the fundamental-mode amplitude calculated by expression (8) (*1*) and the recognition of this amplitude by the neural network during relaxation oscillations (*2*).

In the case of two-mode lasing, the neural network reliably determines the large values of the first mode amplitude and less reliably – small values (Fig. 6). This is seen from the onset of the rise of the curve at $t = 44$ μs and its minimum at $t = 56$ μs. Figure 6b shows the dependence $|b(t)|$ and the recognition results within a small time range in the region $t = 56$ μs. One can see that the NRBF determines sometimes amplitudes that differ from the real value by two discretization intervals. When the values of $|b(t)|$ are close to zero, the NRBF can make even greater mistake. The width of the region where the NRBF identifies the amplitude is determined by the value of $s_m$ in expression (12). However, the decrease in $s_m$ by a factor of 2 – 32 did not improve the situation.

Thus, we can conclude that recognition errors are related to the use of the eigenfunctions in training, which were

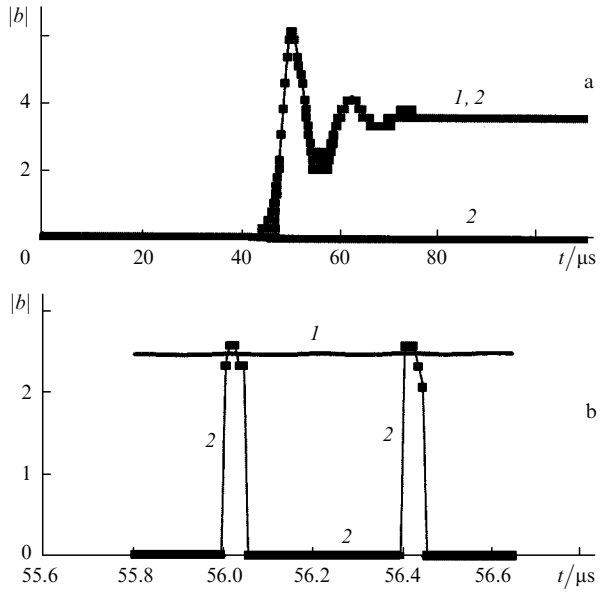


**Figure 6.** Determination of qualitative lasing parameters for the first mode and the amplitude of this mode in the case of two-mode lasing (a) and the NRBF output in the region $t = 56$ μs after the lasing onset (b): the first-mode amplitude calculated by expression (8) (*1*) and the recognition of this amplitude by the neural network during the establishment of two-mode lasing (*2*).

obtained by solving the problem of the development of lasing in the active medium with the instant nonlinear response.

Figure 7 demonstrates the recognition of the presence of the fundamental mode and its amplitude upon two-mode

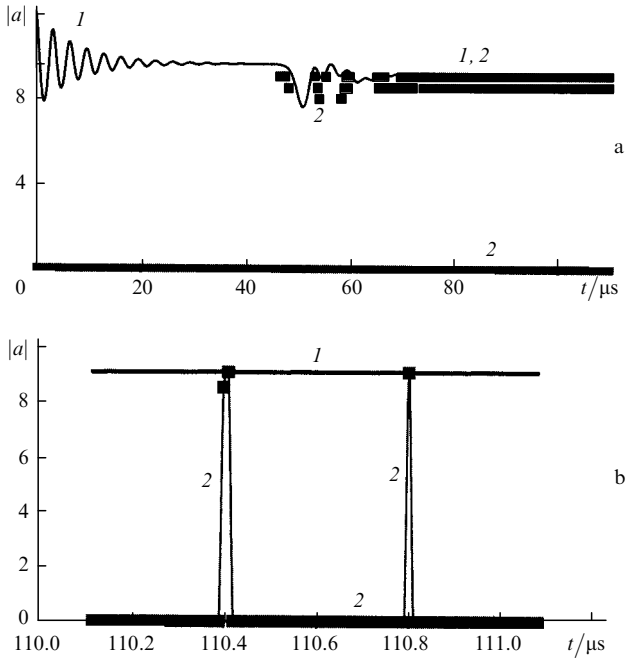


**Figure 7.** Determination of qualitative lasing parameters for the fundamental mode and the amplitude of this mode in the case of two-mode lasing (a) and the NRBF output in the region $t = 110$ μs after the lasing onset (b): the fundamental-mode amplitude calculated by expression (8) (*1*) and the recognition of this amplitude by the neural network in the established two-mode lasing regime (*2*).

lasing by the neural network. One can see that the neural network satisfactorily determined the presence of the fundamental mode, but failed to determine the amplitude of this mode in the interval 44 – 64 μs for large oscillation amplitudes of the first mode. The reason is the same as above. Errors on the recognition of the fundamental-mode amplitude in the case of stationary two-mode lasing were $\sim 7\,\%$.

The neural network used in [5] determined qualitative lasing parameters for each round-trip transit of radiation in the resonator. The NRBF determined quantitative lasing parameters for each round-trip transit in the resonator only for the fundamental mode (Fig. 5). The 'pulsed' character of the recognition of mode amplitudes in the case of two-mode lasing (Figs 6b and 7b) is related to the choice of $\alpha \ll 1$ and to the fact that information on mode phases was neglected during training.

## 5. Conclusions

It has been shown that mode amplitudes can be determined during nonstationary lasing with an error of $5\,\% - 7\,\%$. This error is quite sufficient for laser cutting and welding because the modern models of these processes can give only estimates even when they use complicated equations (for example, in connection with initial approximations [10]). The NRBF provides a compact description of lasing. The total volume of information obtained from the network outputs is less than 1 byte. If this information is delivered to the NRBF with an interval of $10^{-4}$ s, then, as can be easily calculated, the description of 100 hours of continuous lasing will occupy the volume less than 3.6 Gbyte. Such information volumes can be easily processed in modern computers, providing useful data (for example, about the angular position of the beam) for comparison with the results of synchronous recording of technological operations. However, the measurement error of $|a(t)|$ and $|b(t)|$ equal to $5\,\% - 7\,\%$ is insufficient for comparison with the results of analytic studies [1 – 3]. Note in this connection that NRBFs can be further developed because they can be trained by using other sets of the eigenfunctions of the resonator, for example, obtained for distributions $g(x, t_n)$ with the values of $t_n$ corresponding to the local extrema of dependences $|a(t)|$ and $|b(t)|$ (Fig. 2). In addition, the description of the lasing dynamics can be improved by reducing discretization steps $\Delta a$ and $\Delta b$, and the neural network can be supplemented with new groups of neurons, including information on mode phases. Also, the NRBF can be also developed by using neurons with the threshold activation function and employing probability approaches for determining the output values of the network [6].

## References


1. Khanin Ya.I. *Osnovy dinamiki lazerov* (Fundamentals of Laser Dynamics) (Moscow: Nauka, 1999).
2. Bowers M.S., Moody S.E. *Appl. Opt.*, **29**, 3905 (1990).
3. Likhanskii V.V., Napartovich A.P., Sukharev A.G. *Kvantovaya Elektron.*, **22**, 47 (1995) [*Quantum Electron.*, **25**, 40 (1995)].
4. Nesterov A.V., Niz'ev V.G. *Izv. Ross. Akad. Nauk, Ser. Fiz.*, **63**, 2039 (1999).
5. Ledenev V.I. *Kvantovaya Elektron.*, **36**, 933 (2006) [*Quantum Electron.*, **36**, 933 (2006)].
6. Korneev V.V., Gareev A.F., Vasyunin S.V., et al. *Basy dannykh, intellektual'naya obrabotka informatsii* (Databases and Intellectual Data Processing) (Moscow: Izd. S.V. Molgacheva, 2001).
7. Elkin N.N. *Mat. Model.*, **2** (5), 1204 (1990).
8. Anan'ev Yu.A. *Opticheskie rezonatory i lazernye puchki* (Optical Resonators and Laser Beams) (Moscow: Nauka, 1990).
9. Elkin N.N. *Mat. Model.*, **2** (5), 104 (1990).
10. Gross M.S., Black I., Muller W.H. *J. Phys. D: Appl. Phys.*, **36**, 929 (2003).